

George H. Bryan*, Richard Rotunno,
National Center for Atmospheric Research, Boulder, Colorado, USA

and Yongsheng Chen
York University, Toronto, Ontario, Canada

1. INTRODUCTION

In a recent study, Bryan and Rotunno (2009b) (hereafter BR09) investigated the maximum possible intensity of tropical cyclones using an axisymmetric numerical model. They found the maximum azimuthal velocity, $\langle v \rangle_{\max}$, to be sensitive to some parameters in the numerical model that have uncertain values, including: the terminal fall velocity of liquid water; the ratio of the surface exchange coefficients for enthalpy and momentum; and settings in the turbulence parameterization. BR09 found their results to be *most sensitive* to the horizontal turbulence length scale (l_h) in the turbulence parameterization. As shown in Fig. 1, $\langle v \rangle_{\max}$ can vary by more than a factor of three.

In this axisymmetric model, the intensity of radial diffusion is directly proportional to l_h (see BR09 for details). Consequently, radial gradients in scalars and velocity are reduced as l_h is increased. Weaker radial gradients are consistent with weaker intensity by consideration of thermal-wind balance. Unbalanced flow effects are also reduced in axisymmetric models as l_h increases (Bryan and Rotunno 2009a).

A reasonable estimate for l_h is needed because axisymmetric models continue to be used for research and operational forecasting (e.g., Emanuel et al. 2004). However, the most appropriate value of l_h is unclear. There is no quantitative theoretical guidance to help set the value of l_h in axisymmetric models. Previous studies have used values between 3000 m (Rotunno and Emanuel 1987) and 0 m (that is, no turbulence model; Hausman et al. 2006). By comparing model output against observational data, BR09 argued that $l_h \approx 1500$ m is probably the most reasonable value.

A turbulence parameterization for an axisymmetric model must account for all non-axisymmetric structures in tropical cyclones. Conceptually, we consider all non-axisymmetric structures to be *turbulence* from the perspective of the axisymmetric model, and

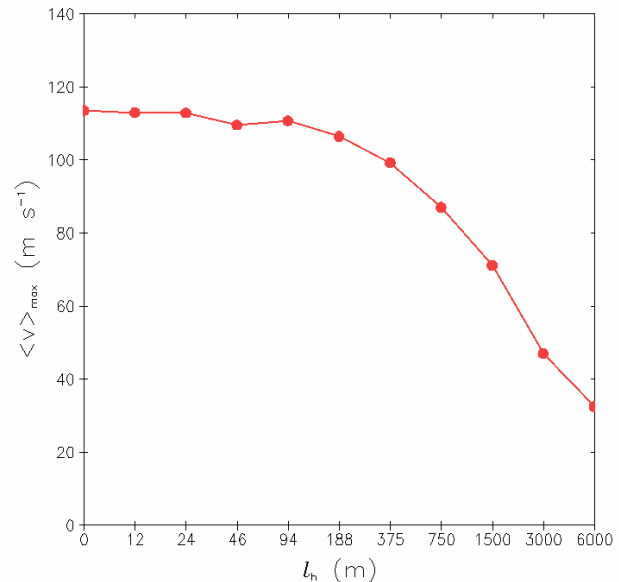


FIG. 1: Maximum azimuthal velocity, $\langle v \rangle_{\max}$, from axisymmetric model simulations that use different values for l_h . [Adapted from Bryan and Rotunno (2009b).]

we consider three types of turbulence herein: 1) *small-scale turbulence*, i.e., the random turbulent eddies within clouds and the planetary boundary layer; 2) *cloud-scale turbulence*, i.e., the deep convective clouds with horizontal scales of $O(1$ km), which includes the so-called “vortical hot towers” (e.g., Montgomery et al. 2006) that have been the focus of much study recently; and, 3) *mesoscale turbulence*, i.e., coherent “eddies” of $O(10$ km) that are predominantly two-dimensional, which includes eyewall mesovortices, asymmetric upper-level outflow jets, etc.

Three-dimensional (3D) numerical models can produce all of these turbulent structures, provided sufficient resolution is used. In the current generation of cloud-scale NWP with horizontal grid spacing of $O(1$ km), the cloud-scale and mesoscale turbulence (types 2 and 3) can be resolved, meaning that only small-scale turbulence (type 1) needs to be param-

*Corresponding author: George H. Bryan, NCAR, 3450 Mitchell Lane, Boulder, CO 80301. Email: gbryan@ucar.edu

eterized. An obvious question arises: is hurricane intensity in 3D simulations with resolution of $O(1 \text{ km})$ also sensitive to turbulence parameterization?

Herein, we analyze the sensitivity of hurricane intensity to parameterized small-scale turbulence in a 3D model. For reference, we also compare against output from the axisymmetric version of the same numerical model.

2. METHODOLOGY

All simulations herein use CM1 (www.mmm.ucar.edu/people/bryan/cm1). The 3D version of the code uses a Cartesian grid, but otherwise uses the same general equations as the axisymmetric model of BR09; that is, the predictive variables are the same (velocity, potential temperature, nondimensional pressure, and mixing ratio), and conservation of mass and energy are carefully considered. The same numerical techniques are used, including: Runge-Kutta time integration; fifth-order flux-form advection (Wicker and Skamarock 2002); and Arakawa-C type grid staggering. We use the simple microphysics and radiation schemes of Rotunno and Emanuel (1987), with a liquid-water fall velocity of 7 m s^{-1} . The surface exchange coefficients are the same as in BR09 (following Rotunno and Emanuel 1987).

Parameterized turbulence in the 3D model uses a traditional downgradient diffusion model. For this study, eddy viscosity is separated into a value for the horizontal direction (ν_h) and one for the vertical direction (ν_v) (as in BR09), but for the 3D model they are determined as follows:

$$\nu_h = l_h^2 S_h \quad \text{and} \quad \nu_v = l_v^2 (S_v^2 - N_m^2)^{1/2} \quad (1)$$

where l_h and l_v are (specified) turbulence length scales in the horizontal and vertical directions, respectively, S_h and S_v are deformation in the horizontal and vertical directions, respectively, where

$$S_h^2 = 2 \left(\frac{\partial u}{\partial x} \right)^2 + 2 \left(\frac{\partial v}{\partial y} \right)^2 + \left(\frac{\partial u}{\partial y} + \frac{\partial v}{\partial x} \right)^2, \quad (2)$$

$$S_v^2 = 2 \left(\frac{\partial w}{\partial z} \right)^2 + \left(\frac{\partial u}{\partial z} + \frac{\partial w}{\partial x} \right)^2 + \left(\frac{\partial v}{\partial z} + \frac{\partial w}{\partial y} \right)^2, \quad (3)$$

and N_m^2 is the squared Brunt-Väisälä frequency for moist air, which is calculated the same way as in BR09. If $N_m^2 > S_v^2$ then ν_v is set to zero.

The 3D domain is $3000 \text{ km} \times 3000 \text{ km} \times 25 \text{ km}$. Constant horizontal grid spacing of 1 km is used over a $128 \text{ km} \times 128 \text{ km}$ region in the center of the domain. Outside this region, horizontal grid spacing is smoothly increased to reduce computational costs

Table 1: Results from simulations that use different values for l_v (with $l_h = 1500 \text{ m}$), where $\langle v \rangle_{\max}$ is maximum azimuthally averaged azimuthal velocity, r_{\max} is the radius where $\langle v \rangle_{\max}$ is located, and z_{\max} is the height where $\langle v \rangle_{\max}$ is located.

l_v (m)	$\langle v \rangle_{\max}$ (m s^{-1})	r_{\max} (km)	z_{\max} (km)
25	66	19	0.6
50	67	20	0.6
100	67	22	0.9
200	62	23	1.1
400	65	22	1.4

(as in BR09). Maximum horizontal grid spacing is 15 km at the sides of the domain (1500 km away from the hurricane eye). Vertical grid spacing ($\Delta z = 250 \text{ m}$) is constant everywhere.

The initial conditions are identical to those in BR09 except small-amplitude random temperature perturbations are placed into the initial vortex to encourage development of 3D motions. The sea-surface temperature is $26.1 \text{ }^\circ\text{C}$. Each simulation is integrated from $t = 0$ to $t = 12$ days using constant (specified) values of l_h and l_v for the entire simulation.

For 3D simulations, the center of the tropical cyclone is determined (for the purposes of post-processing) by the gridpoint that maximizes calculations of azimuthally averaged azimuthal velocity. We found this to be a more reliable method than other techniques, such as using lowest pressure or maximum vertical vorticity, which tended to identify strong convective cells.

3. SENSITIVITY OF 3D SIMULATIONS TO SMALL-SCALE TURBULENCE

As in BR09, we find that varying l_v (with l_h fixed) does not have much affect on maximum azimuthally averaged azimuthal velocity $\langle v \rangle_{\max}$. For example, results with $l_h = 1500 \text{ m}$ are listed in Table 1; $\langle v \rangle_{\max}$ varies by only a few m s^{-1} . However, the structure of tropical cyclones is impacted by l_v . Specifically, as l_v increases: the depth of the inflow layer increases; the magnitude of radial inflow decreases; and the radius of maximum winds increases slightly (Table 1).

In contrast, maximum intensity in 3D simulations is strongly affected by l_h : see Fig. 2. In fact, $\langle v \rangle_{\max}$ is as sensitive to l_h in the 3D model (black) as it is in the axisymmetric model (red), with a factor of three difference between $l_h = 0$ and 6000 m .

Compared to the axisymmetric model, $\langle v \rangle_{\max}$ is systematically lower in the 3D model by $\sim 20\%$. Our analysis of this difference is preliminary, but it is likely related to the mesoscale turbulence that

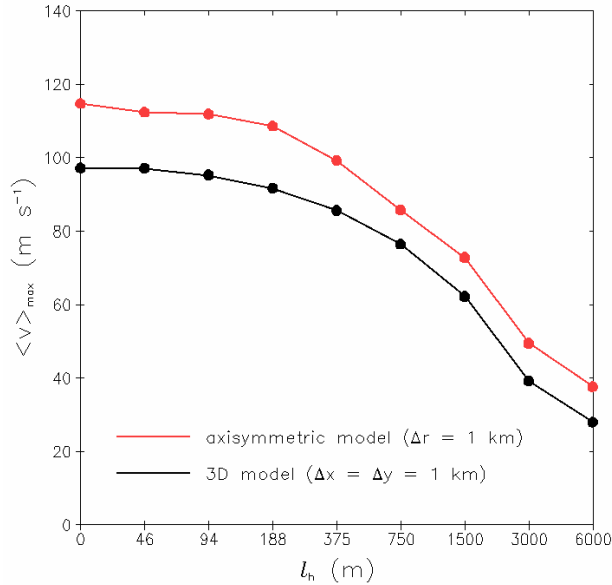


FIG. 2: Maximum azimuthally averaged azimuthal velocity, $\langle v \rangle_{\max}$, from the axisymmetric model (red) and the three-dimensional model (black). All simulations use $l_v = 200$ m.

the 3D model can produce (but the axisymmetric model cannot). Features resembling eyewall mesovortices (e.g., Montgomery et al. 2002) form along the eye/eyewall interface; they ultimately act to diffuse (mix) in the radial direction. In fact, as previous studies have found (e.g., Hausman et al. 2006), axisymmetric numerical models can produce potential-vorticity profiles that are unstable to combined baroclinic-barotropic instability. Schubert et al. (1999) found that azimuthal velocity decreased when this instability was removed by mesoscale turbulence. The results of our modeling study are consistent. Profiles of azimuthally averaged azimuthal velocity $\langle v \rangle$ are shown in Fig. 3a for simulations without any parameterized turbulence in the horizontal direction (i.e., for $l_h = 0$). Flow is nearly zero in the eye with the axisymmetric model, but, in contrast, the 3D model has $\langle v \rangle$ increasing monotonically with radius in the eye (Fig. 3a). The difference in the two profiles is consistent with angular momentum being mixed between the eye and the eyewall, and with the eye being “spun up” at the expense of angular momentum at the inner-edge of the eyewall. Profiles of $\langle v \rangle$ are similar outside the eyewall ($r > 20$ km) in both models. A similar result is obtained when parameterized turbulence is included (Fig. 3b).

Intensification is shown via time-series of $\langle v \rangle_{\max}$ in Fig. 4. We find that the axisymmetric model intensifies faster than the 3D model for low values of l_h (Fig. 4a); this result suggests that the mesoscale turbulence (e.g., eyewall mesovortices) and the cloud-

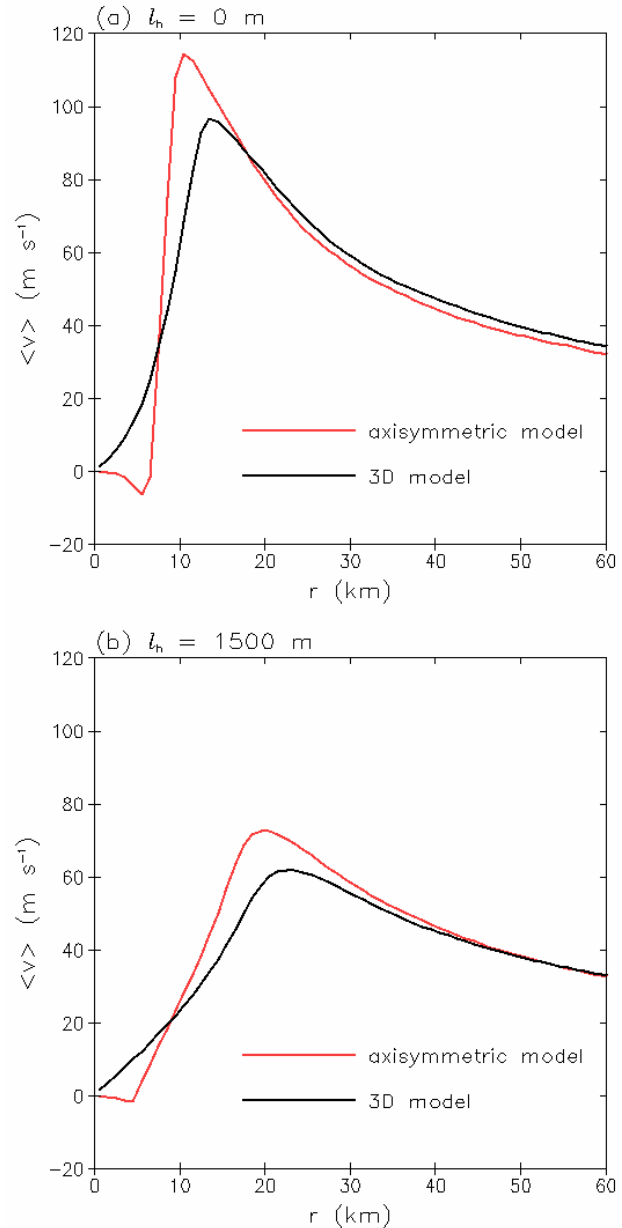


FIG. 3: Azimuthally averaged azimuthal velocity, $\langle v \rangle$, at 1.1 km AGL from simulations using $l_v = 200$ m: (a) $l_h = 0$ m; and (b) $l_h = 1500$ m. Axisymmetric model output is in red, and 3D model output is in black.

scale turbulence (e.g., “vortical hot towers”) that are produced by the 3D model (but not the axisymmetric model) act to reduce intensification rate as well as maximum intensity. For $l_h > \sim 1000$ m, the axisymmetric and 3D models have similar intensification rates (Fig. 4b), although maximum intensity is weaker in 3D simulations.

For the early intensification period (the first three days of these simulations), the intensification rate in axisymmetric model simulations is affected little by l_h (cf. red lines in Fig. 4). In contrast, the 3D model intensifies faster as l_h increases (for $l_h < \sim 1000$ m). For example, the $l_h = 1500$ m simulation reaches 40 m s^{-1} about 14 hours earlier than the $l_h = 0$ simulation (cf. black lines in Fig. 4).

At first glance, these results may seem to suggest that parameterized turbulent diffusion acts directly to increase intensification rate. However, this diffusion also weakens mesoscale and cloud-scale turbulence. As an example, a snapshot of convective updrafts is shown in Fig. 5. When l_h is increased the updrafts tend to be broader and generally weaker (i.e., w_{\max} is smaller). Vertical vorticity in convective updrafts is also much weaker as l_h increases (see maximum/minimum values of ζ in Fig. 5).

We have conducted additional simulations using different soundings and sea-surface temperatures to determine whether these conclusions hold for other environments. When using $l_h = 0$ we find that 3D simulations always intensify slower than axisymmetric simulations, and the delay is proportional to environmental CAPE. When using the Jordan (1958) hurricane sounding and $T_s = 28 \text{ }^\circ\text{C}$, the 3D simulation needs 23 additional hours to reach $\langle v \rangle_{\max} = 50 \text{ m s}^{-1}$ compared to the axisymmetric model (not shown).

Our findings are consistent with a similar study (using coarser resolution) by Yang et al. (2007). However, our results seem to be at odds with the study by Emanuel (1997) who found, using a simple model, that increases in radial diffusion of momentum increased intensification rate but did not affect maximum intensity. The different results may be attributable to the neglect of radial diffusion of heat by Emanuel (1997). (Our model diffuses both momentum and heat.) In future work, we will investigate whether our results change when turbulent diffusion of heat is neglected or held fixed.

Several recent studies have concluded that cloud-scale turbulence (i.e., “vortical hot towers”) increases maximum intensity and helps increase intensification rate [e.g., Montgomery et al. (2006, 2009)]. One possible explanation for the opposite conclusion herein is that, possibly, our 3D model has different numerical diffusion than our axisymmetric model, especially considering the different underlying grids (cylindrical

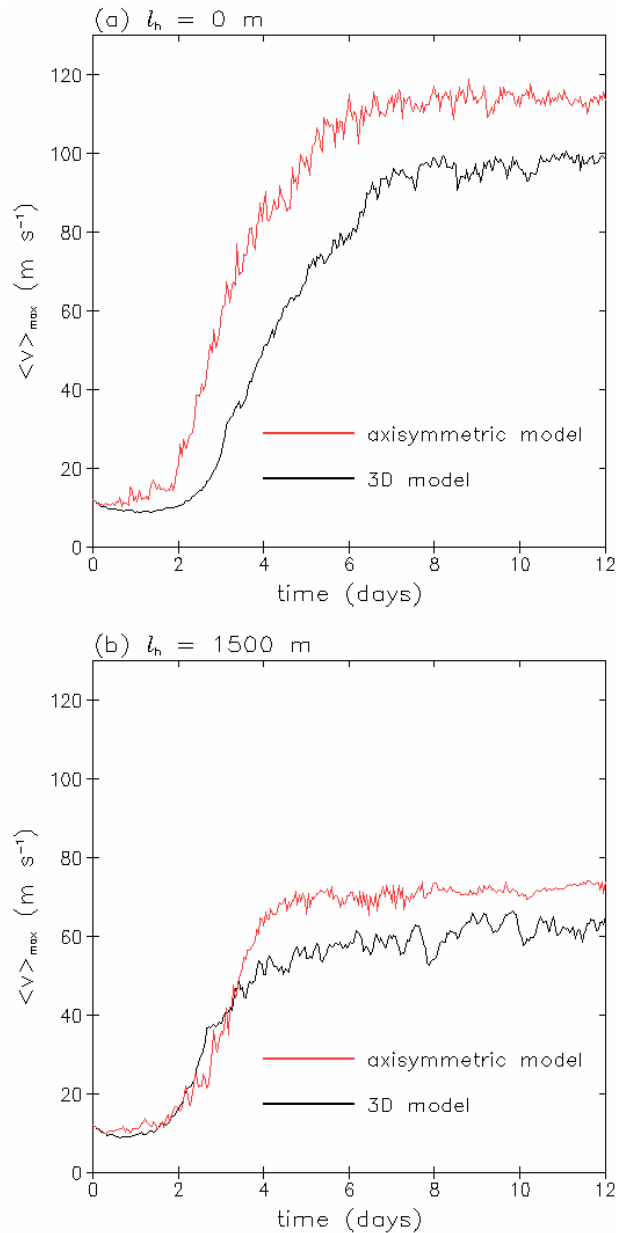


FIG. 4: Plots of $\langle v \rangle_{\max}$ over time from the axisymmetric model (red) and the 3D model (black) for (a) $l_h = 0$ m and (b) $l_h = 1500$ m. All cases use $l_v = 200$ m.

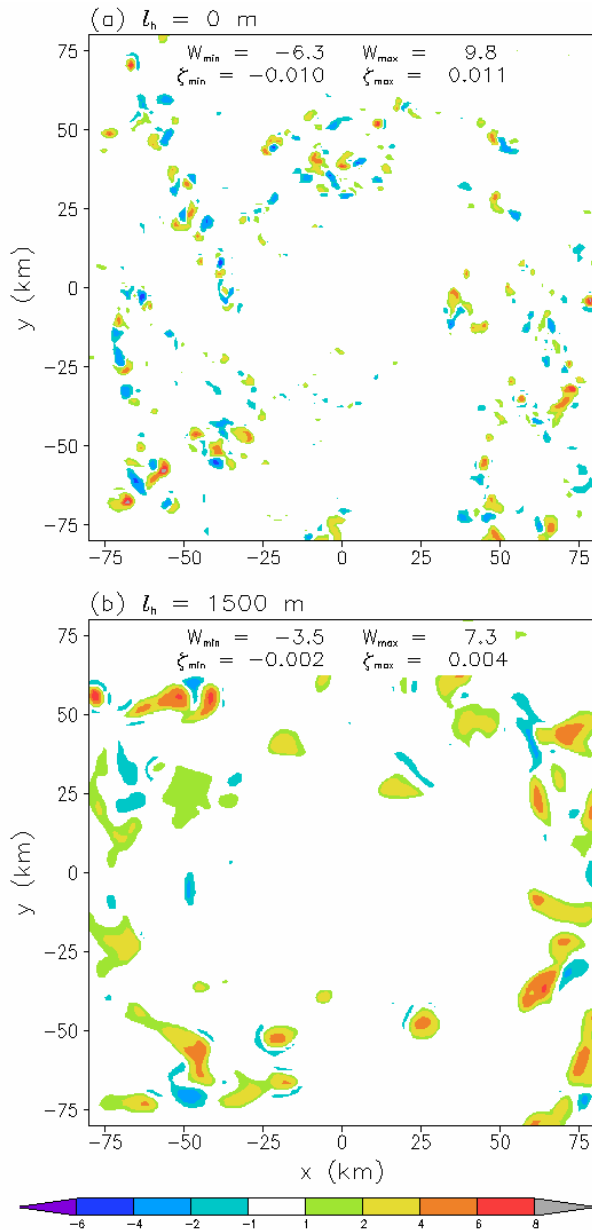


FIG. 5: Vertical velocity at 5 km AGL and $t = 2$ days for (a) $l_h = 0$ m and (b) $l_h = 1500$ m.

vs rectangular). We are exploring this topic further, and one method would be to conduct 3D simulations using a cylindrical grid (as in Rotunno 1984).

On the other hand, analyses of turbulent fluxes caused by eyewall mesovortices and “vortical hot towers” in the present simulations are consistent with a deleterious affect on intensification. Specifically, the mesoscale and cloud-scale features have positive turbulent fluxes of entropy in the radial direction, which act to reduce the radial gradient in entropy. Weaker radial gradients in entropy are consistent with weaker, more slowly developing cyclones (e.g., Emanuel 1997; Bryan and Rotunno 2009b). Our findings are also consistent with recent idealized studies on the effects of asymmetric convection on mean hurricane intensity (e.g., Nolan and Grasso 2003; Nolan et al. 2007).

4. CONCLUDING REMARKS

These preliminary results, using $\Delta x = \Delta y = 1$ km and $\Delta z = 250$ m, show that 3D numerical simulations are sensitive to parameterized turbulence in the horizontal. Similar to results from our axisymmetric model, we find that $\langle v \rangle_{\max}$ can be changed by a factor of three when the turbulence length scale l_h is varied between 0 and 6000 m.

For reference, we note that these results should not be specific to this numerical model (CM1). The horizontal turbulence parameterization used herein is standard and is used in other numerical models. For example, the Advanced Research WRF model (ARW) uses an identical parameterization for horizontal turbulence; called the “horizontal Smagorinsky first order closure”,¹ this turbulence parameterization is recommended for real-data cases, according to the ARW User’s Guide.² In ARW, the value of l_h is a function of horizontal grid spacing (Δ_h) by the relation

$$l_h = 0.25 \times \Delta_h. \quad (4)$$

Hence, users of the ARW model will have $l_h = 1000$ m when using 4 km horizontal grid spacing, but $l_h = 250$ m when using 1 km grid spacing. Our analysis (Fig. 2) suggests that an increase in maximum intensity could occur by changing Δ in the ARW model; this conclusion is supported by the simulations of Rotunno et al. (2009) (for $\Delta > 100$ m). It seems that intensity changes in resolution sensitivity tests using ARW might be more attributable to changes in l_h than to changes in horizontal grid spacing alone.

¹Using `km_opt = 4` in the `namelist.input` file

²See <http://www.mmm.ucar.edu/wrf/users/pub-doc.html>

Acknowledgements

The National Center for Atmospheric Research is sponsored by the National Science Foundation. Computing resources were provided by the Shared Hierarchical Academic Research Computing Network (SHARCNET:www.sharcnet.ca) and Compute/Calcul Canada.

REFERENCES

- Bryan, G. H., and R. Rotunno, 2009a: Evaluation of an analytical model for the maximum intensity of tropical cyclones. *J. Atmos. Sci.*, **66**, 3042–3060.
- Bryan, G. H., and R. Rotunno, 2009b: The maximum intensity of tropical cyclones in axisymmetric numerical model simulations. *Mon. Wea. Rev.*, **137**, 1770–1789.
- Emanuel, K., C. DesAutels, C. Holloway, and R. Korty, 2004: Environmental control of tropical cyclone intensity. *J. Atmos. Sci.*, **61**, 843–858.
- Emanuel, K. A., 1997: Some aspects of hurricane inner-core dynamics and energetics. *J. Atmos. Sci.*, **54**, 1014–1026.
- Hausman, S. A., K. V. Ooyama, and W. H. Schubert, 2006: Potential vorticity structure of simulated hurricanes. *J. Atmos. Sci.*, **63**, 87–108.
- Jordan, C. L., 1958: Mean soundings for the West Indies area. *J. Meteor.*, **15**, 91–97.
- Montgomery, M. T., M. E. Nicholls, T. A. Cram, and A. B. Saunders, 2006: A vortical hot tower route to tropical cyclogenesis. *J. Atmos. Sci.*, **63**, 355–385.
- Montgomery, M. T., N. V. Sang, R. K. Smith, and J. Persing, 2009: Do tropical cyclones intensify by WISHE? *Quart. J. Roy. Meteor. Soc.*, **135**, 1697–1714.
- Montgomery, M. T., V. A. Vladimirov, and P. V. Denissenko, 2002: An experimental study on hurricane mesovortices. *J. Fluid Mech.*, **471**, 1–32.
- Nolan, D. S., and L. D. Grasso, 2003: Nonhydrostatic, three-dimensional perturbations to balanced, hurricane-like vortices. Part II: Symmetric response and nonlinear simulations. *J. Atmos. Sci.*, **60**, 2717–2745.
- Nolan, D. S., Y. Moon, and D. P. Stern, 2007: Tropical cyclone intensification from asymmetric convection: Energetics and efficiency. *J. Atmos. Sci.*, **64**, 3377–3405.
- Rotunno, R., 1984: An investigation of a three-dimensional asymmetric vortex. *J. Atmos. Sci.*, **41**, 283–298.
- Rotunno, R., Y. Chen, W. Wang, C. Davis, J. Dudhia, and G. J. Holland, 2009: Large-eddy simulation of an idealized tropical cyclone. *Bull. Amer. Meteor. Soc.*, **90**, 1783–1788.
- Rotunno, R., and K. A. Emanuel, 1987: An air-sea interaction theory for tropical cyclones. Part II: Evolutionary study using a nonhydrostatic axisymmetric numerical model. *J. Atmos. Sci.*, **44**, 542–561.
- Schubert, W. H., M. T. Montgomery, R. K. Taft, T. A. Guinn, S. R. Fulton, J. P. Kossin, and J. P. Edwards, 1999: Polygonal eyewalls, asymmetric eye contraction, and potential vorticity mixing in hurricanes. *J. Atmos. Sci.*, **56**, 1197–1223.
- Wicker, L. J., and W. C. Skamarock, 2002: Time splitting methods for elastic models using forward time schemes. *Mon. Wea. Rev.*, **130**, 2088–2097.
- Yang, B., Y. Wang, and B. Wang, 2007: The effect of internally generated inner-core asymmetries on tropical cyclone potential intensity. *J. Atmos. Sci.*, **64**, 1165–1188.